Supporting information

Ion Parking in Native Mass Spectrometry

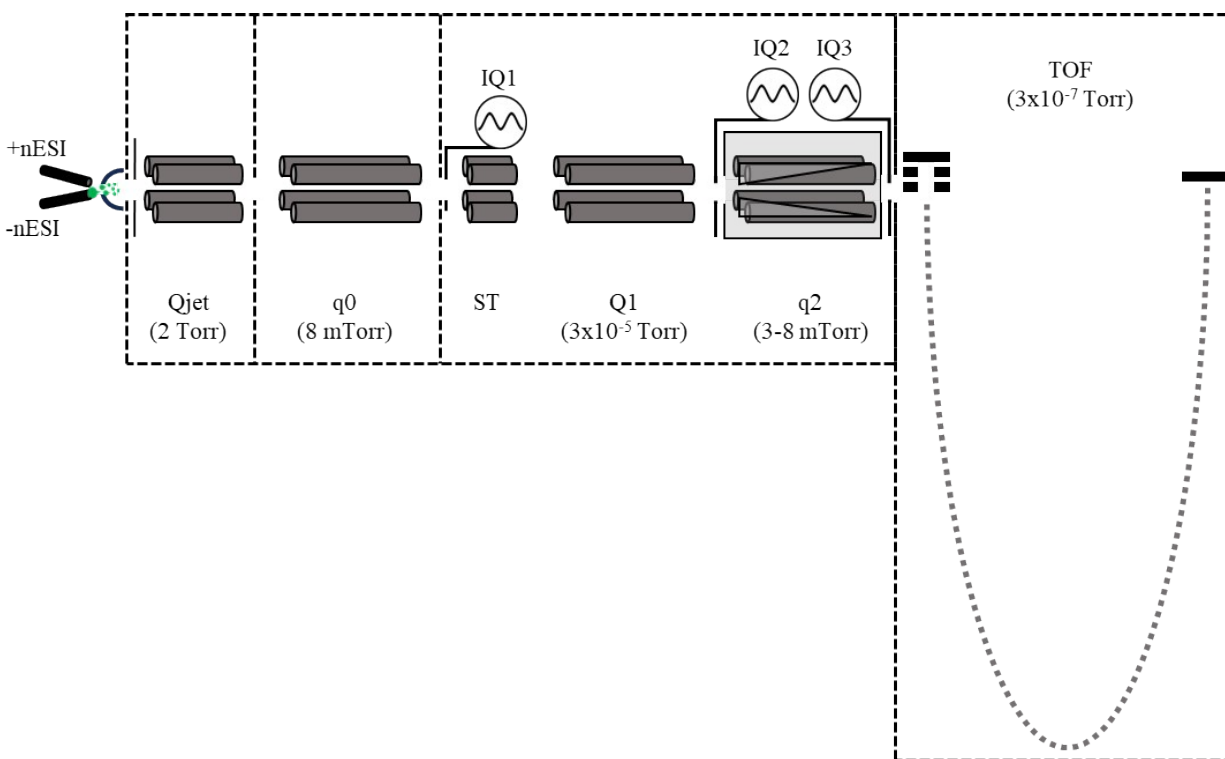Nicolas J. Pizzala, Jay S. Bhanot, Ian J. Carrick, Eric T. Dziekonski, Scott A. McLuckey*

Department of Chemistry
Purdue University
West Lafayette, IN, USA 47907-2084

*Address reprint requests to:

Dr. Scott A. McLuckey
560 Oval Drive
Department of Chemistry
Purdue University
West Lafayette, IN 47907-2084, USA
Phone: (765) 494-5270
Fax: (765) 494-0239
E-mail: mcluckey@purdue.edu

Table of Contents

Figure S1 - Instrument schematic for the modified SCIEX Triple TOF 5600. Dual emitters, which are sequentially pulsed to allow for the admission of oppositely-charged ions, are depicted near the entrance to the atmosphere-vacuum interface.

Ion parking model:

Frequency spacing between adjacent charge states.

The *m/z*-dependent frequencies of ion motion are given by:

$$\omega_{n,u} = \frac{(2n \pm \beta_u)\Omega}{2}$$

(S1)

where n is an integer, u is the x- or y-dimension, and Ω is the angular frequency of the drive RF.[1] The so-called fundamental secular frequency is that for which n=0, i.e.:

$$\omega_{0,u} = \frac{\beta_u \Omega}{2} = 2\pi f_{0,u}$$

(S2)

where $f_{0,u}$ is the fundamental secular frequency in Hz. β_u can be approximated from the dimensionless a and q parameters of the Mathieu equation, the solutions of which describe ion motion in electrodynamic quadrupole ion traps:

$$\beta_u \cong \sqrt{a_u + \frac{q_u^2}{2}}$$

(S3)

which is valid for $q_u < 0.4$.[1] The a_u parameter in a linear quadrupole ion trap is given by:

$$a_u = \frac{8zeU}{m_i r_o^2 \Omega^2}$$

(S4)

and the q_u parameter is given by:

$$q_u = \frac{4zeV_{RF}}{m_i r_o^2 \Omega^2}$$

(S5)

where z is the unit charge of the ion, m_i is the mass of the ion, r_o is the inscribed radius of the quadrupole rod array, U is the amplitude of the quadrupolar DC, and V_{RF} is the 0-p amplitude of the drive RF used to confine ions.[2] Ion parking is generally performed in the absence of a quadrupolar DC potential (i.e., a_u=0). Hence, equation (3) can be simplified to:

$$\omega_{0,u} = \frac{q_u \Omega}{2\sqrt{2}}$$

(S6)

The secular frequency can also be written as:

$$\omega_{0,u} = \frac{4zeV_{RF}\Omega}{2\sqrt{2}m_i r_0^2 \Omega^2} = \frac{\sqrt{2}zeV_{RF}}{m_i r_0^2 \Omega}$$

(S7)

From the standpoint of parking a selected charge state from all others for a given protein, the frequency spacing between charge states is relevant. The difference in the fundamental secular frequencies of adjacent charge states can be estimated by:

$$\Delta\omega_{0,u,z-state} = \omega_{0,u,z+1} - \omega_{0,u,z} \cong \frac{\sqrt{2}(z+1)eV_{RF}}{m_i r_0^2 \Omega} - \frac{\sqrt{2}zeV_{RF}}{m_i r_0^2 \Omega} \cong \frac{\sqrt{2}eV_{RF}}{m_i r_0^2 \Omega}$$

(S8)

(Recall that $\Delta\omega_{0,u,z\text{-state}} = 2\pi\Delta f_{0,u,z\text{-state}}$.) The masses of the ions in adjacent charge states are not strictly equal, as they differ by the mass of the species responsible for the charge difference (usually a proton). However, this mass difference is negligible relative to the mass of the native complex.

Mechanisms of ion parking. The preceding discussion relates the dependence of ion frequency on the trapping parameters and the *m/z* values of the ions, which is key to ion parking using resonance excitation. The following part of the discussion describes how trapping parameters and *m/z* values of the ions relate to the mechanism of ion parking using resonance excitation. The basis for ion parking is the the selective inhibition of an ion/ion reaction rate, R_{I-I}, given by:

$R_{I-I} = k_c[\text{cations}][\text{anions}]$ (S9)

where k_c is the rate constant and [cations] and [anions] are the respective concentrations of the reactants. The reaction can be inhibited by reducing the numbers of reactants, reducing the physical overlap of the reacting ion populations, thereby reducing their effective concentrations (i.e., the effective [cations] and [anions] decreases when they do not occupy overlapping regions of space), and/or by reducing k_c. The reduction of ion cloud overlap has been demonstrated using a dipolar DC potential across opposing electrodes in a 3-D ion trap[3] and by resonance excitation of ions in 2-D[4] and 3-D[5] electrodynamic ion traps. The rate constant can be reduced by increasing the relative velocity of the reactants. Under typical ion trap conditions, the rate constant for an ion/ion reaction can be approximated by the Thomson three-body model:[6]

$$k_c = v_{rel,I-I} \pi \left[\frac{z_1 z_2 e^2}{\mu_{I-I} v_{rel,I-I}^2} \right]^2$$

(S10)

in which the $v_{rel,i/i}$ is the relative velocity of the oppositely charged ions, z_1 and z_2 are the elementary charges of the cation and anion, respectively, and μ_{I-I} is the reduced mass of the collision partners:

$$\mu_{I-I} = \frac{m_{cation}m_{anion}}{m_{cation} + m_{anion}}$$

(S11)

Eq. 10 shows that the rate constant is dependent upon the squares of the charges of the reactant ions and is inversely related to the third power of the relative velocity. Hence, acceleration of one or both of the reactants can, in principle, result in a marked decrease in the reaction rate constant via the rate constant dependence on relative velocity. In the absence of resonance excitation and assuming both ions are thermalized from collisions with the bath gas, the mean $v_{rel,I-I}$ can be approximated as:

$$\overline{v_{rel,I-I,T}} = \sqrt{\frac{8k_BT}{\pi\mu_{I-I}}}$$

(S12)

where k_B is the Boltzmann constant. As the mass of the analyte ion increases, the reduced mass approaches that of the reagent ion. In other words, the light ion has a much greater velocity and therefore has a greater influence on relative velocity. The result is that the relative velocity becomes less sensitive to resonance excitation of the analyte ion as the mass of the analyte ion increases. For selective rate inhibition, the analyte ion of the charge state of interest must be accelerated since acceleration of the reagent ion would lead to the diminution of the reaction rates of all ions. If the ions are not in thermal equilibrium, the square of the relative velocity is given by[7]:

$$v_{rel,I-I}^2 = v_{anion}^2 + v_{cation}^2 - 2v_{anion}v_{cation}cos\theta_{CM}$$

(S13)

Where v_{anion} and v_{cation} are the anion and cation velocities, respectively, and θ_{CM} is the center-of-mass scattering angle. For estimating the average relative velocity, the average θ_{CM} can be taken as 90^0,[8] leading to:[9]

$$\overline{v_{rel,I-I}}^2 \approx \overline{v_{anion}}^2 + \overline{v_{cation}}^2$$

(S14)

The average velocity of the thermalized reagent anion is given by:

$$\overline{v_{anion}} = \sqrt{\frac{8k_BT}{\pi m_{anion}}}$$

(S15)

where m_{anion} is the anion mass. The average velocity of the thermalized cation is given by:

$$\bar{v}_{cation} = \sqrt{\frac{8k_BT}{\pi m_{cation}}}$$

(S16)

where m_{cation} is the cation mass. The average velocity of the cation undergoing resonance excitation can be determined from its average kinetic energy:

$$\bar{v}_{cation} = \sqrt{\frac{2\bar{KE}}{m_{cation}}}$$

(S17)

The average kinetic energy of an ion undergoing resonance excitation includes both its initial thermal kinetic energy and the additional kinetic energy resulting from acceleration by the dipolar oscillatory filed. While the latter is determined by several variables, the maximum kinetic energy, KE_{max}, is limited by the product of the ion charge and the pseudopotential well-depth, D_u:[10,11]

$$KE_{max} \cong zeD_u$$

(S18)

where D_u for a linear electrodynamic ion trap can be approximated by:[12]

$$D_u = \frac{q_u V_{RF}}{4}$$

(S19)

The maximum average cation velocity that can be reached before ion ejection, therefore, can be estimated as:

$$\bar{v}_{cation,max} \cong \sqrt{\frac{2zeD_u}{m_{cation}}}$$

(S20)

The above relationship can be used with relation relations (14) and (15) to estimate the maximum relative velocity, $v_{rel,I\text{-}I,max}$, value for each analyte charge state that can be achieved via resonance excitation for a given set of trapping conditions:

$$\bar{v}_{rel,I-I,max} \cong \sqrt{\frac{8k_BT}{\pi m_{anion}}} + \sqrt{\frac{2zeD_u}{m_{cation}}}$$

(S21)

The ratio of the ion/ion reaction rate constants with and without resonance excitation can then be estimated by:

$$\frac{k_{c,parking}}{k_c} = \left(\frac{v_{rel,I-I,T}}{v_{rel,I-I,max}}\right)^3 = \left(\frac{\sqrt{\frac{8k_BT}{\pi\mu_{I-I}}}}{\left(\sqrt{\frac{8k_BT}{\pi m_{anion}}}+\sqrt{\frac{2zeD_u}{m_{cation}}}\right)}\right)^3 \tag{S22}$$

Ion cloud size. As indicated in **Figure 1** of the main text, the reduction of the rate constant of an ion/ion reaction via an increase in relative ion velocity is increasingly difficult as the mass of the analyte ion increases relative to that of the reagent ion. The other mechanism for ion rate reduction is to minimize ion overlap as the cation ion cloud oscillates back and forth. The product of charge and well-depth, zeD_u, also plays a role in limiting the extent to which ion overlap can be minimized using resonance excitation. We have recently used a model originally described by Trypogeogos, Foot, et al.[13,14] for estimating the size of an ion cloud in the x-y plane in a linear quadrupole ion trap using a simple harmonic oscillator analogy.[15] The model treats an ion as a harmonic oscillator with a spring constant, κ, that determines the root-mean-squared extent of the ion cloud in dimension u at temperature T, u_T, i.e.:

$$\frac{1}{2}k_BT = \frac{1}{2}\kappa u_T^2 \tag{S23}$$

where k_B is the Boltzmann constant. The spring constant is estimated by:

$$\kappa = m\omega_0^2 \cong \frac{2zeV_{RF}}{r_0^2}\cdot\frac{q_u}{8} = \frac{zeD_u}{r_0^2} \tag{S24}$$

where ω_0 is the natural frequency of the harmonic oscillator, which we take as the fundamental secular frequency of the ion in question. Substituting Equation 24 in Equation 23 and solving for u_T yields:

$$u_T \cong \left(\frac{k_BTr_0^2}{zeD_u}\right)^{1/2} \tag{S25}$$

which, using the relationships for D_u (Eq. 19) and q_u (Eq. 5), expands to:

$$u_T \cong \left(\frac{m_ik_BTr_0^4\Omega^2}{z^2e^2V_{RF}^2}\right)^{1/2} \tag{S26}$$

When u_T approaches r_0, the stored ion cloud begins to undergo ion evaporation as the high energy tail of the ion kinetic energy distribution exceeds D_u.

The ion cloud sizes of the anions and cations in an ion parking experiment are relevant in establishing the extent to which they can be separated under resonance excitation conditions. If it is assumed that the ion cloud under resonance excitation conditions moves coherently and that the clouds of oppositely charged ions are of sufficiently low densities that they have minimal influence over each other's size, the amplitude of the ion cloud oscillation, A_{AC}, must exceed the sum of the radii of the cation and anion clouds for complete separation of the ion clouds:

$$A_{AC} > u_{T,cation} + u_{T,anion}$$

(S27)

When the sum of the A_{ac} and u_T,cation approaches r_0, resonance excitation will result in cation loss as the cation cloud begins to contact the rods. Hence, r_0 is the limit for the sum of A_{AC} and $u_{T,cation}$:

$$r_0 > A_{AC} + u_{T,cation}$$

(S28)

Alternatively, the oscillatory amplitude due to resonance excitation is:

$$A_{AC} < r_0 - u_{T,cation}$$

(S29)

Charge state resolution. Another important figure of merit of an ion parking experiment is the specificity (or resolution) with which ion parking can be performed. Given the fact that the frequency spacings of adjacent charge states are constant under typical reaction conditions and that the secular frequencies decrease with *m/z*, it is of interest to examine the extent to which off-resonance power absorption by adjacent charges states might complicate parking ions into a single charge state of interest. A simple model to examine the effect of the resonance excitation signal on the amplitude of oscillation of ions of different secular frequencies is based on regarding the resonance excitation experiment in an ion trap as a driven harmonic oscillator with damping. Such an approach has long been used to model secular ion motion in ion traps. The maximum oscillatory amplitude, $A_{max,AC}$, of a damped harmonic oscillator with a natural frequency, ω_0, driven by an external frequency, ω_{AC}, is given by:[16]

$$A_{max,AC} = \frac{aV_{AC}ze}{2r_0 m_i \sqrt{c^2\omega_{AC}^2 + \left(\omega_{AC}^2 - \omega_0^2\right)^2}}$$

(S30)

where "a" is a term to account for the fact that the dipolar excitation is applied to round rods rather than to flat plates (a=0.798[17,18]), V_{AC} is the p-p amplitude of the dipolar AC applied to opposing rods, and c is the term to account for damping resulting from collisions with a bath gas. Many ion trap modelling papers[19] base the determination of collision frequency on polarization theory and usually use the familiar Langevin formalism. A convenient consequence of the use of the polarization model is that the collision rate constant is velocity independent, which leads to a

constant damping factor. However, the Langevin ion-induced dipole model assumes the ion to be a point-charge, which is most appropriate for relatively small ions. However, the sizes of the ions encountered in native MS generally have cross-sections much larger than those determined via the Langevin formalism. We therefore have used a combined hard-sphere + ion-induced dipole model for determining the collision frequency and assume an elastic model for momentum transfer. The damping term, c, is determined from:

$$c = R_{coll}\left(\frac{m_g}{m_g + m_{cation}}\right)$$

(S31)

Where m_g is the bath gas mass and R_{coll} is the ion/bath gas collision frequency. R_{coll} is taken as the sum of the hard-sphere collision rate plus the ion-induced dipole collision rate based on the charge state of the ion,

$$R_{coll} = n_g\sigma_{h-s}v_{rel,I-M} + n_g\sigma_L v_{rel,I-M}$$

(S32)

where n_g is the bath gas number density, σ_{h-s} is the hard-sphere cross-section, which can be approximated, or taken directly, from reported ion-mobility measurements, and σ_L is the Langevin cross-section:

$$\sigma_L = \frac{2\pi ze}{(4\pi\varepsilon_0)v_{rel,I-M}}\left(\frac{\alpha}{\mu_{I-M}}\right)^{\frac{1}{2}}$$

(S33)

where ε_0 is vacuum permittivity, α is the electronic polarizability of the bath gas (1.710 Å^3, or 1.90x10^{-40} C-m^2-V^{-1} in SI units, for N$_2$[20]), and μ is the reduced mass of the ion/bath gas pair:

$$\mu_{I-M} = \frac{m_{cation}m_g}{m_{cation} + m_g}$$

(S34)

The $v_{rel,I-M}$ terms cancels in the Langevin contribution to the collision rate so that the Langevin rate constant, k_L:

$$k_L = \frac{2\pi ze}{(4\pi\varepsilon_0)}\left(\frac{\alpha}{\mu_{I-M}}\right)^{\frac{1}{2}}$$

(S35)

can replace the $\sigma_L v_{rel,I-M}$ term in relation (32):

$$R_{coll} = n_g\sigma_{h-s}v_{rel,I-M} + n_g k_L$$

(S36)

The hard-sphere collision rate, on the other hand, is dependent on $v_{rel,I-M}$. For a given charge state of an ion under fixed trapping conditions, the maximum relative velocity, $v_{rel,I-M,max}$, is limited by the product of the charge and well-depth, in analogy with the $v_{rel,I-I,max}$ discussed above. A similar

relationship can be used to approximate this value using the mass of the bath gas in place of the mass of the anion:

$$\overline{v}_{rel,I-M,max} \cong \sqrt{\frac{8k_BT}{\pi m_g}} + \sqrt{\frac{2zeD_u}{m_{cation}}} = \sqrt{\frac{8k_BT}{\pi m_g}} + \frac{\sqrt{2}zeV_{RF}}{m_{cation}r_0\Omega} \tag{S37}$$

The value of c (i.e., the damping factor) is dependent on $v_{rel,I-M}$, which depends on the amplitude of the resonance excitation voltage. For a given analyte ion, the range of c values, c_{min} to c_{max}, can be estimated by determining c_{min} in the absence of resonance excitation, as estimated by:

$$c_{min} \cong \left(n_g\sigma_{h-s}\sqrt{\frac{8k_BT}{\pi\mu_{I-M}}} + n_gk_L\right)\left(\frac{m_g}{m_g + m_{cation}}\right) \tag{S38}$$

which uses the value of the average relative velocity of the ion-neutral pair at temperature T, $\sqrt{\frac{8k_BT}{\pi\mu_{I-M}}}$, for $v_{rel,I-M,T}$, the minimum relative velocity, and determining c_{max} at the maximum extent of resonance excitation prior to ejection from the ion trap, as reflected by $\overline{v}_{rel,I-M,max}$:

$$c_{max} \cong \left(n_g\sigma_{h-s}\left(\sqrt{\frac{8k_BT}{\pi m_g}} + \frac{\sqrt{2}zeV_{RF}}{m_{cation}r_0\Omega}\right) + n_gk_L\right)\left(\frac{m_g}{m_g + m_{cation}}\right) \tag{S39}$$

List of symbols:

|	
$\omega_{n,u}$	secular frequencies (rad/s) of motion in dimension u
$\omega_{0,u}$	fundamental secular frequency (rad/s)
$\Delta\omega_{0,u,z\text{-state}}$	approximate difference in fundamental secular frequency between adjacent z-states (rad/s)
$f_{0,u}$	fundamental secular frequency (Hz)
$\Delta f_{0,u,z\text{-state}}$	approximate difference in fundamental secular frequency between adjacent z-states (Hz)
β_u	beta value in dimension u (dimensionless)
Ω	ion trap drive frequency (rad/s)
$f_{0,u}$	fundamental secular frequency (Hz)
a_u	a-Mathieu parameter for dimension u (dimensionless)
q_u	q-parameter for dimension u (dimensionless)
z	ion unit charge
e	fundamental charge (C)
U	quadrupolar DC (V)
m_i	ion mass (kg)
m_{cation}	cation mass (kg)
m_{anion}	anion mass (kg)
m_g	bath gas mass (kg)
r_0	ion trap inscribed radius (m)
V_{RF}	amplitude of the quadrupolar radio-frequency (RF) potential ($V_{0\text{-}p}$)
$R_{I\text{-}I}$	ion-ion reaction rate (s^{-1})
k_c	ion-ion capture rate constant in the absence of parking
$k_{c,parking}$	ion-ion capture rate constant for an ion being parked
$v_{rel,I\text{-}I}$	relative velocity of the ion-ion reaction reactants
$v_{rel,I\text{-}M}$	relation velocity of the ion-bath gas pair
$\mu_{I\text{-}I}$	reduced mass of the ion-ion pair
$\mu_{I\text{-}M}$	reduced mass of the ion-bath gas pair
T	temperature (K)
$\bar{v}_{rel,I-I,T}$	average relative velocity of the ion-ion pair at temperature T (m/s)
$\bar{v}_{rel,I-M,T}$	average relative velocity of the ion-bath gas pair at temperature T (m/s)
$\bar{v}_{rel,I-I}^{\,2}$	square of the average ion-ion relative velocity (m/s)
$\bar{v}_{anion}^{\,2}$	square of the average anion velocity (m/s)
$\bar{v}_{cation}^{\,2}$	square of the average cation velocity (m/s)
$\bar{v}_{cation,max}$	average maximum cation velocity (m/s)
k_B	Boltzmann constant
$\bar{KE}$	average kinetic energy of the cation
KE_{max}	maximum kinetic energy of the cation
D_u	pseudo-potential well-depth in dimension u (V)
κ	spring constant of the ion trap
u_T	ion cloud radius in dimension u at temperature T

A_{AC}	amplitude of the ion oscillatory amplitude under resonance excitation
$A_{max,AC}$	maximum amplitude of ion oscillation under resonance excitation
c	damping factor (s^{-1})
R_{coll}	ion/bath gas collision rate (s^{-1})
n_g	number density of the bath gas
$\sigma_{h\text{-}s}$	hard-sphere collision cross-section
σ_L	ion-induced dipole collision cross-section (Langevin)
α	bath gas polarizability
$4\pi\varepsilon_0$	permittivity of free space
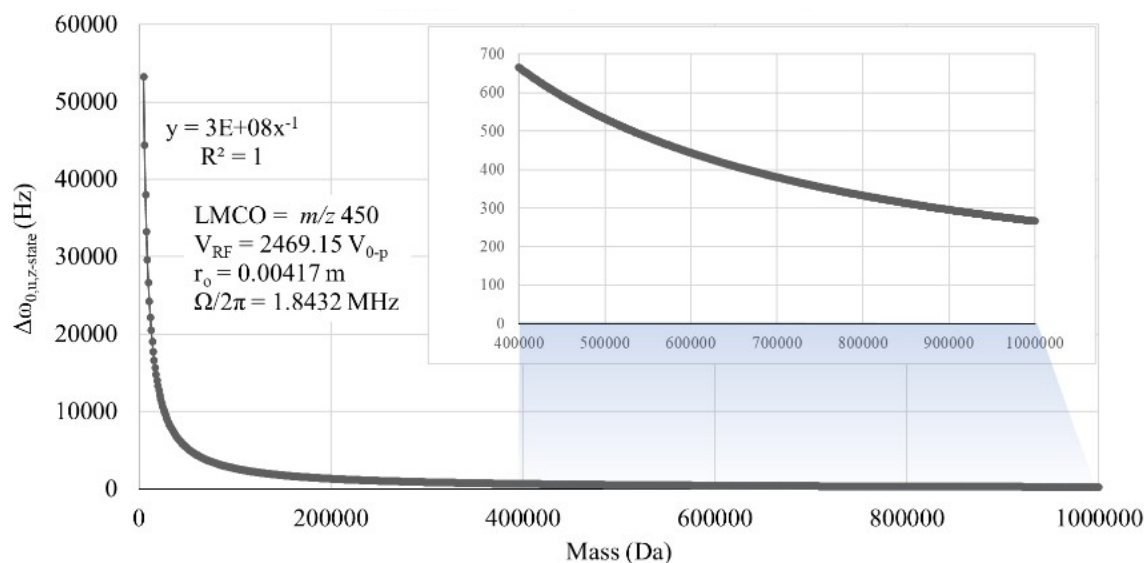
Figure S2. Plot of the frequency spacing between adjacent charge states (Hz) as a function of ion mass (Da) under trapping conditions listed in the figure insert.
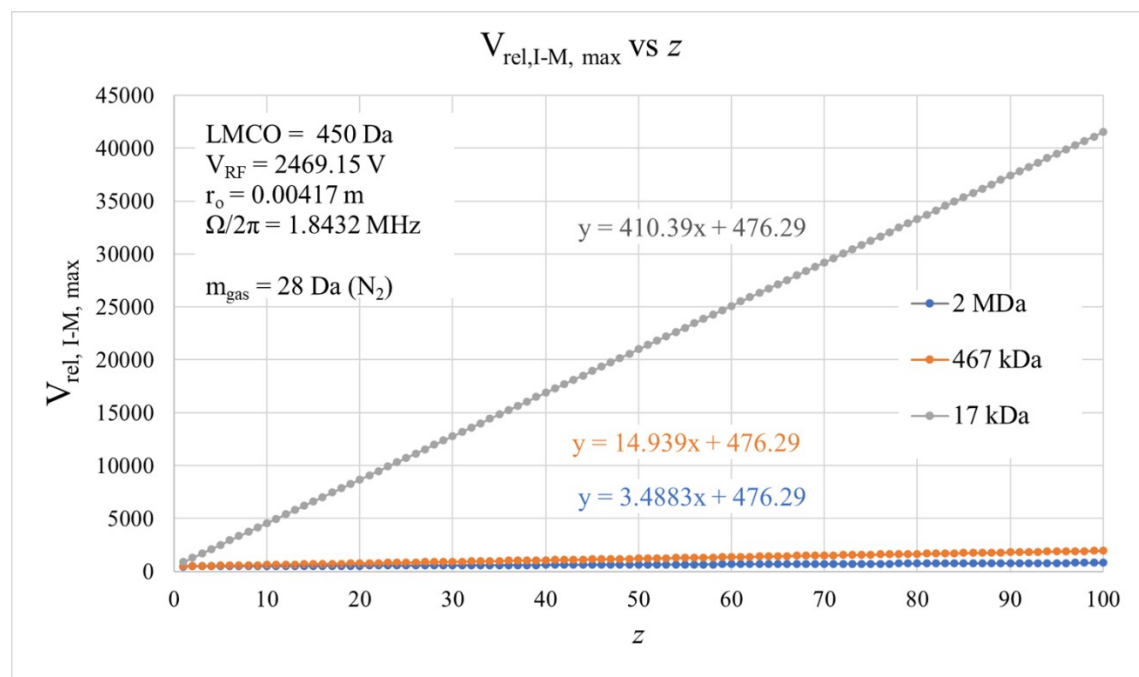
Figure S3 - Plot of the maximum relative ion velocity for an ion-molecule reaction under the storage conditions indicated in the figure for ions of 17 kDa (grey), 467 kDa (orange), and 2 MDa (blue) using Eq. 19 of the main text (SI Eq. 36).
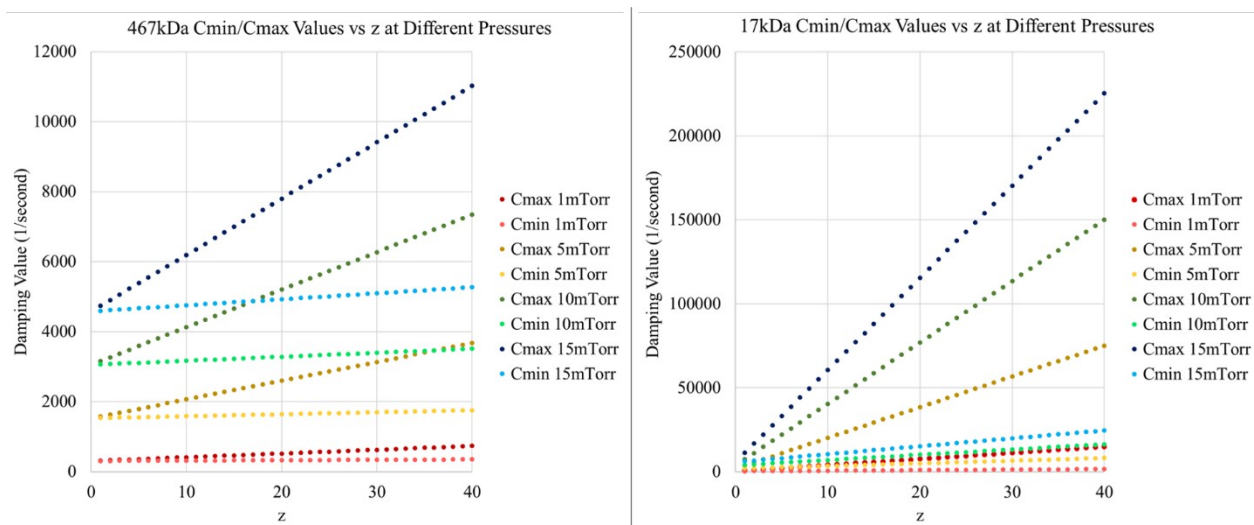
Figure S4 - Plots of c_{min} (light shade) and c_{max} (dark shade) as a function of z for ions of mass 467 kDa (**a**) and 17 kDa (**b**) at nitrogen bath gas pressures 1 (red), 5 (yellow), 10 (green), and 15 (blue) mTorr.

References

1   Fulford, J.E.; Nhu-Hoa, D.; Hughes, R.J.; March, R.E.; Bonner, R. F.; Wong, G.J. Radio-frequency mass selective excitation and resonant ejection of ions in a three-dimensional quadrupole ion trap. *J. Vac. Sci. Tech.* **1980**, *17*, 829-835.

2   March, R.E. An Introduction to Quadrupole Ion Trap Mass Spectrometry. *J. Mass Spectrom.* **1997**, *32* (4), 351–369.

3   Grosshans, P.B.; Ostrander, C.M.; Walla, C.A. Method and Apparatus to Control Charge Neutralization Reactions in Ion Traps. U.S. Patent 6,570,151 B1.

4   Campbell, J.L., Le Blanc, J.C.Y. "Targeted ion parking for the quantitation of biotherapeutic proteins: Concepts and preliminary data." *J. Am. Soc. Mass. Spectrom.* **2010**, *21*, 2011-2022.

5   McLuckey, S. A.; Reid, G. E.; Wells, J. M. Ion Parking during Ion/Ion Reactions in Electrodynamic Ion Traps. *Anal. Chem.* **2002**, *74* (2), 336–346.

6   McLuckey, S. A.; Stephenson, J. L.; Asano, K. G. Ion/Ion Proton-Transfer Kinetics: Implications for Analysis of Ions Derived from Electrospray of Protein Mixtures. *Anal. Chem.* **1998**, *70* (6), 1198–1202.

7   Tolmachev, A.V.; Chernusevich, I.V.; Dodonov, A.F.; Standing, K.G. A collisional focusing ion guide for coupling an atmospheric pressure ion source to a mass spectrometer. *Nucl. Instrum. Methods in Phys. Res. B* **1997**, *124*, 112-119.

8   Covey, T.; Douglas D.J. Collision Cross Sections for Protein Ions. *J. Am. Soc. Mass Spectrom.* **1993**, *4*, 616-623.

9   Collings, B.A.; Stott, W.R.; Londry, F.A. Resonant Excitation in a Low-Pressure Linear Ion trap. *J. Am. Soc. Mass Spectrom.* **2003**, *14*, 622-634.

10   Wuerker, R.F.; Shelton, H.; Langmuir, R.V. Electrodynamic Containment of Charged Particles. *J. Appl. Phys.* **1959**, *30*, 342-349.

11   Major, F.G.; Dehmelt, H.G. Exchange-Collision Technique for the rf Spectroscopy of Stored Ions. *Phys. Rev.* **1968**, *170*, 91-107.

12   Douglas, D.J.; Frank, A.J.; Mao, D. Linear ion traps in mass spectrometry. *Mass Spectrom. Rev.* **2005**, *24*, 1-29.

13   Trypogeorgos, D.; Foot, C.J. Co-trapping different species in ion traps using multiple radio frequencies. *Phys. Rev.* A **2016**, *94*, 023609.

14   Foot; C.J., Trypogeorgos, D.; Bentine, D.E.; Gardner, A.; Keller, M. Two-frequency operation of a Paul trap to optimize confinement of two species of ions. *Int. J. Mass Spectrom.* **2018**, *430*, 117-125.

15   Bhanot, J.S.; Fabijanczuk, K.C.; Abdillahi, A.M.; Chao, H.-C.; Pizzala, N.J.; Londry, F.A.; Dziekonski, E.T.; Hager, J.W.; McLuckey, S.A. Adaptation and Operation of a Quadrupole/Time-of-Flight Tandem Mass Spectrometer for High Mass Ion/Ion Reaction Studies. *Int. J. Mass Spectrom.* **2022**, *478*, 116874.

16   Xu, W.; Chappell, W.J.; Ouyang, Z. Modeling of ion transient response to dipolar AC excitation in a quadrupole ion trap. *Int. J Mass Spectrom.* **2011**, *308*, 49-55.

17   Douglas, D. J.; Konenkov, N. V. Mass Selectivity of Dipolar Resonant Excitation in a Linear Quadrupole Ion Trap. *Rapid Commun. Mass Spectrom.* **2014**, *28* (5), 430–438. https://doi.org/10.1002/rcm.6795.

18   Michaud, A. L.; Frank, A. J.; Ding, C.; Zhao, X.; Douglas, D. J. Ion Excitation in a Linear Quadrupole Ion Trap with an Added Octopole Field. *J. Am. Soc. Mass Spectrom.* **2005**, *16* (6), 835–849. https://doi.org/10.1016/j.jasms.2005.02.006.

19   Goeringer, D.E.; Whitten, W.B.; Ramsey, J.M.; McLuckey, S.A.; Glish, G.L. Theory of High Mass Resolution Achieved via Resonance Ejection in the Quadrupole Ion Trap. *Anal. Chem.* **1992**, *64*, 1434-1439.

20   Olney, T.N.; Cann, N.M.; Cooper, G.; Brion, C.E. Absolute scale determination for photoabsorption spectra and the calculation of molecular properties using dipole sum rules. *Chem. Phys.* **1997**, *223*, 59-98.